Constraints on Mantle Anelasticity from SLR Tidal Estimates

John Wahr and David Benjamin
Department of Physics and Cooperative Institute for Research in Environmental Sciences
University of Colorado, Boulder, CO 80309-0390, USA
Shailen Desai
Jet Propulsion Laboratory, California Institute of Technology
4800 Oak Grove Drive, Pasadena, CA 91109, USA

Abstract

Satellite Laser Ranging (SLR) measurements of the Earth's gravity field can be used to solve for solid Earth tides. We use those solutions to place constraints on anelasticity in the Earth's mantle at periods of 12 hours and 18.6 years. The results imply that the anelastic parameter Q is smaller for those tides than for seismic waves. We interpret this as evidence that Q is frequency dependent. We find that the frequency dependence suggested by the SLR measurements is reasonably consistent with laboratory measurements, but inconsistent with seismic observations.

Introduction

The Sun and Moon exert gravitational forces on the Earth. These forces not only cause the Earth's orbital motion, but they also cause the Earth to deform. The Moon, for example, exerts a greater force on the side of the Earth closer to it than on the side further away. This differential force is called the tidal force. It causes the Earth to deform, creating a tidal bulge that stretches out both towards and away from the Moon. The bulge follows the Moon as it orbits the Earth, while the Earth rotates through the bulge at one cycle per day. The geometry is such that the tidal deformation, referred to as the body tide, is split into three frequency bands: a semi-diurnal band, with frequencies of 2 c/d modulated by the much longer periods of the lunar orbit (e.g., 13.7 d, 27.6 d, 18.6 years, etc.); a diurnal band, with frequencies of 1 c/d modulated by those same lunar periods; and the long-period band, consisting of just the lunar orbital periods alone. The situation is similar for the tides caused by the Sun.

The amplitude and phase of the body tide depend on the internal rheology of the Earth. The smaller the shear modulus, for example, the greater the deformation. Furthermore, energy dissipation (e.g., anelasticity) causes the maximum deformation to occur slightly after the Moon (or Sun) has passed overhead. Thus, observations of the tidal deformation can provide information about the Earth's interior. This is a situation, after all, where the driving force can be modeled extremely accurately. It is determined by the orbital motions of the Earth and Moon and by the solar and lunar masses, all of which are well known.

But the situation is complicated by the oceans. The tidal force acts on them as well, causing ocean tides. The ocean tides push on the underlying solid Earth and deform it, causing a load tide. The amplitude and phase of the load tide, like those of the body tide, depend on the Earth's rheology. But the load tide is of less practical use for constraining large-scale properties of the Earth's deep interior. This is partly because it is much easier to model the gravitational force from the Sun and Moon (which is what drives the body tide) than it is to model ocean tides (which are what drive the load tide). And it is also partly because the body tide persists further down into the Earth's interior than does the load tide.

Both the body tide and the load tide affect tidal observations. Since body tides and ocean tides are caused by the same force, they occur at the same frequencies, and so the body and load tides cannot be separated using a single tidal observation. Because ocean tides are difficult to model, attempts to learn about the Earth's interior from body tide observations are always degraded to some extent by uncertainties in the load tide.

Satellite Laser Ranging (SLR) solutions for tidal variations in the gravity field, have an advantage in this respect over most ground-based observations. SLR measurements, like tidal measurements from any technique, can be used to solve only for a linear combination of body and load tides. But whereas ground-based measurements provide estimates of tidal deformation at discrete points on the Earth's surface, SLR observations provide estimates of tidal effects on specific spherical harmonic coefficients of the gravity field. The advantage is that while the load tide at any tidal frequency tends to be distributed among all spherical harmonics, the body tide is almost entirely represented by a single spherical harmonic. Thus, the ratio of load tide to body tide in SLR solutions for that one spherical harmonic, tends to be relatively small.

The tidal force-per-mass is the gradient of a scalar function, $V(r,\theta,\phi)$, referred to as the tidal potential, where (r,θ,ϕ) are geocentric spherical coordinates (radius, co-latitude, Eastward longitude). The time-dependence of V occurs at a set of discrete frequencies, grouped into the semi-diurnal, diurnal, and long-period bands described above. Let ω be one of these frequencies. The contribution to V at that frequency has the form [see *Cartwright and Tayler*, 1971]:

$$V = Re\,[H(\omega)(r^2/a^2)Y_2^m(\theta,\phi)e^{i\omega t}] \qquad (1)$$

where Y_2^m is the complex spherical harmonic of degree 2 and order m, $H(\omega)$ is the tidal amplitude at this frequency, a is the Earth's radius, Re denotes the real part, and m = 2 for semi-diurnal tides, = 1 for diurnal tides, and = 0 for long-period tides.

Because the solid Earth is nearly spherically symmetric, and because the dynamical effects of its diurnal rotation are small, the body tide deformation induced by (1) causes a perturbation in the Earth's external gravitational potential that can be described using the same spherical harmonic:

$$\delta = Re\,[k(\omega)\,H(\omega)(a^3/r^3)Y_2^m(\theta,\phi)e^{i\omega t}] \qquad (2)$$

Here, $k(\omega)$ is the gravitational Love number at the frequency ω, and is complex for an anelastic Earth. SLR can recover tidal amplitudes and phases for this single Y_2^m term, and so can be used to constrain $k(\omega)$.

SLR solutions for Y_2^m also include contributions from the load tide. The spatial dependence of the load tide is more complicated, involving spherical harmonics of all degrees and orders. But load tide contributions to spherical harmonics other than Y_2^m are irrelevant for these SLR solutions. So to interpret those solutions it is only necessary to know one spherical harmonic component of the ocean tide. Furthermore, because this component has a global spatial scale (the wavelength of Y_2^m is 20,000 km), it is one of the easier components to determine accurately.

In this paper we place constraints on mantle anelasticity using SLR observations of two tides: the semi-diurnal tide M_2 and the 18.6-year long-period tide. This requires a model of the Y_2^2 component of the M_2 ocean tide, and of the Y_2^0 component of the 18.6-year ocean tide. The contribution from the load tide to each of these components is computed using an expression similar to (2):

$$\delta_{load} = Re\,[\{1+k'(\omega)\}\,H'(\omega)(a^3/r^3)\,Y_2^m(\theta,\phi)e^{i\omega t}] \qquad (3)$$

where H' is the Y_2^m component of the gravitational potential caused by the ocean tide, k' is the load Love number, and the factor "1" in "1+ $k'(\omega)$" represents the direct gravitational potential of the ocean tide itself. SLR is sensitive to the sum of (2) and (3). The SLR observations thus provide a constraint on a linear combination of the Love numbers k and k', which can be used to place bounds on anelasticity. Typically, H' is on the order of a few percent of H. Thus, the linear combination is dominated by k, so that it is the body tide that provides most of the anelastic information.

Ocean tide models

To use tidal observations to learn about the solid Earth, it is necessary to model the ocean tide. For our application, it is necessary only to determine H' in (3). There are two general strategies employed in ocean tide modeling: (1) using altimeter measurements of tidal amplitudes, and (2) solving the differential equations describing tidal dynamics. Each method has its characteristic advantages and weaknesses, and many of the most accurate models use a combination of both.

In this paper we discuss only the M_2 and 18.6-year tides. For M_2 we use the SLR solutions from *Ray et al* [2001]. They estimated H' by averaging results from four M_2 ocean tide models, each of which relied on a combination of dynamic modeling and TOPEX/Poseidon (T/P) altimeter data. Tidal components with global spatial scales are determined more accurately from altimeter data than from dynamical modeling, so that most of the strength of the Y_2^2 solutions in each model comes from the T/P data.

Using T/P data is not a viable option for modeling the 18.6-year tide. The altimeter has been in orbit for only about half a cycle for this tide, which is not long enough to separate the tidal signal from the non-tidal, decadal-scale variability in the ocean. Instead, we make the assumption that the 18.6-year tide is in equilibrium with the tidal potential. This is equivalent to assuming the barotropic response time of the ocean is much faster than 18.6-years. It implies that tidal currents are negligible, as are the Coriolis and inertial forces induced by those currents. There is then a balance between the pressure forces caused by changes in sea level, and the gravitational forces caused by the Moon and Sun, the solid Earth tides, and the sea level perturbation itself. An equilibrium tidal response for a period this long is supported by dynamical arguments [see, for example, *Carton*, 1983], and is consistent with T/P observations that show the fortnightly tide is close to equilibrium, and the monthly tide is closer still [*Desai and Wahr*, 1999].

Mantle anelasticity

There is a large body of evidence that when material in the Earth's mantle is deformed, energy is dissipated. The mechanisms responsible for this dissipation are not well understood, and are almost certain to be different in different frequency regimes and for different stress levels. The dissipation occurs almost entirely in shear energy; dissipation of bulk energy (associated with changes in volume) appears to be negligible for most applications.

Shear dissipation is represented by the quality factor, $Q(\omega)$, defined so that for deformation at frequency ω, the fraction of energy lost per cycle is $2\pi/Q$. Suppose, as seems likely, that dissipation within the Earth's mantle is caused by an absorption band process, meaning that the dissipation occurs at relaxation times spread continuously over some time interval. For forcing at periods within this interval, it can be shown [see, for example, *Dahlen and Tromp*, 1998] that under reasonably general conditions the frequency dependence of Q is of the form

$$Q(\omega) = Q_0 \, (\omega / \omega_0)^{\alpha} \tag{4}$$

where Q_0 is the value of Q at some reference frequency ω_0 within the absorption band, and α depends on the details of the physical process causing the absorption. If α could be determined from observations, it would presumably provide information about that process.

Because of the principle of causality [see, for example, the discussion of the Kramers-Kronig relation in *Dahlen and Tromp,* 1998], dissipative mechanisms must also cause dispersion: i.e., frequency dependence of wave speeds. Let $Q(r, \omega)$ be the quality factor for shear dissipation at radius r and frequency ω. If the frequency dependence of Q is given by (4) where α is small, and if the attenuation is small enough that $Q(r,\omega) >> 1$, then it can be shown that the perturbation in the shear modulus, $\delta\mu$, is

$$\delta\mu(r, \omega) \; \mu_0 (r) \; [\, 2/\pi Q(r) \; \{1 - (\omega_0/\omega)^{\alpha(r)}\} + i \; (\omega_0/\omega)^{\alpha(r)} \,] / Q_0 (r) \tag{5}$$

where $\mu_0(r)$ is the real part of the shear modulus at radius r and frequency ω_0. The imaginary part of (5) represents dissipation, and the frequency dependence of the real part represents dispersion. In the assumed absence of bulk dissipation, the bulk modulus (the other rheological parameter besides μ, and not shown here) is real and frequency independent.

For tides, the dissipative terms in (5) cause a phase lag between the forcing and the response, and the dispersive terms cause the in-phase tidal amplitudes to depend on frequency. Put in another way, dissipation causes the Love numbers k and k' to have imaginary parts, and dispersion causes their real parts to be frequency dependent. If $\alpha \neq 0$, then the imaginary parts of k and k' depend on frequency too, through the frequency dependence of Q. And by taking the limit of (5) as $\omega \to 0$, it can be shown that there is dispersion even if $\alpha = 0$.

There is evidence of dissipation within the Earth's mantle at periods of seconds to tens of minutes from seismology; and at periods of several thousand years and longer from observations of post-glacial rebound and processes related to mantle convection. The physical mechanisms in these two cases are undoubtably different. At periods of thousands of years and longer the relevant processes probably involve either diffusion or dislocation creep. For seismic waves the anelasticity may be related to the opening and closing of pre-existing cracks in the medium.

This difference in mechanisms manifests itself as a difference in α. For post-glacial rebound, for example, the Earth's mantle is usually modeled as a Maxwell solid, in which $\alpha = 1$. In contrast, seismic observations require no frequency dependence of Q, so that $\alpha = 0$ within the seismic band. This latter conclusion, though, is in conflict with most laboratory measurements of Q at seismic and ultra-seismic periods, that imply that α in the upper mantle is likely between 0.15 and 0.40 [see, for example, *Gribb et al*, 1998]. We return to this point below.

There is little information about anelasticity at periods between 1 hour and thousands of years. Observations of the Chandler Wobble period and damping have been used to constrain the anelasticity at a period of 14 months [see, e.g., *Smith and Dahlen,* 1981]. There have been several studies that use the fortnightly and monthly tidal variations of the length-of-day to constrain anelasticity at those periods [see, e.g., *Dickman and Nam,* 1998; *Defraigne and Smits,* 1999]. And SLR observations have been used to bound the anelasticity at periods of 12 hours and 18.6 years, through observations of the M_2 and 18.6-year tides [see, e.g., *Eanes*, 1995; *Ray et al*, 2001]. It is these SLR constraints that we revisit in this paper.

SLR Observations

We use the results of *Ray et al* [2001] for the M_2 Love number. *Ray et al* determined the Y_2^2 component of the body tide from SLR observations, modeling the Y_2^2 component of the load tide using the ocean models described above, and assuming the phase lag of the load Love number k' is about the same as the phase lag of the body tide Love number k (the phase lag $= atan(-k_i/k_r)$, where k_i and k_r are the imaginary and real parts of k). *Ray et al* [2001] concluded that the phase lag in the M_2 body tide Love number is $0.20^o \pm 0.05^o$. They were not able to place a useful constraint on the Love number amplitude. But their results imply that the real and imaginary parts are related by: $k_i = -k_r \cdot \tan(0.20^o \pm 0.05^o) \approx k_r \cdot (-0.0035 \pm 0.0009)$.

For the 18.6-year Love number, we use two estimates. One is from *Eanes* [1995], who used SLR data to solve for an 18.6-year variation in Y_2^0, removed the 18.6-year load tide using the equilibrium ocean tide model of *Ray and Cartwright* [1994], and assumed the load Love number k' is unaffected by anelasticity. We have modified *Eanes*' result slightly, by using the equilibrium ocean tide model of *Desai and Wahr* [1995] instead of *Ray and Cartwright* [1994], and by increasing the uncertainties in both k_r and k_i by adding (in quadrature) an ocean tide error assumed to be 5% of the equilibrium value. We obtain real and imaginary parts for k of: $k_r = 0.3358 \pm 0.0060$ and $k_i = -0.0045 \pm 0.0117$.

Eanes [1995] used SLR data taken between 1976 and 1995. Subsequent SLR observations show an anomalous feature in the Y_2^0 component of the Earth's gravity field that began sometime during 1997, consisting of a pronounced change in slope lasting for 3-4 years, followed by a recovery toward the pre-1997 conditions over the next couple of years [see *Cox et al*, 2003; this volume]. As noted by *Cox et al*, this feature affects solutions for the 18.6-year tide. This effect is illustrated in Figure 1. We used *Cox et al*'s monthly Y_2^0 values for 1979-2002 (which we refer to as CABC; provided by C. Cox, 2003) and simultaneously fit in-phase and out-of-phase 18.6-year tidal components, seasonally-varying components, and a linear trend. We performed these fits for a variety of time intervals, each one beginning in 1979, but ending at times that varied between 1994 and the end of 2002. The equilibrium ocean tide model of *Desai and Wahr* [1995] was removed, and the residuals were converted to the body tide Love number estimates presented in Figure 1. Also shown, as asterisks, are *Eanes*'s [1995] estimates. The error bars on the CABC results are the sum (added in quadrature) of the 1-σ formal errors from the fit, and an ocean tide error assumed to be 5% of the equilibrium value. Note that there are differences between our CABC solutions for the time span ending in the middle of 1995, and *Eanes*'s results for that same time span. This may be partly because *Eanes* used data for a few years prior to 1979, and partly because of differences in the solution processes adopted to produce the monthly Y_2^0 values.

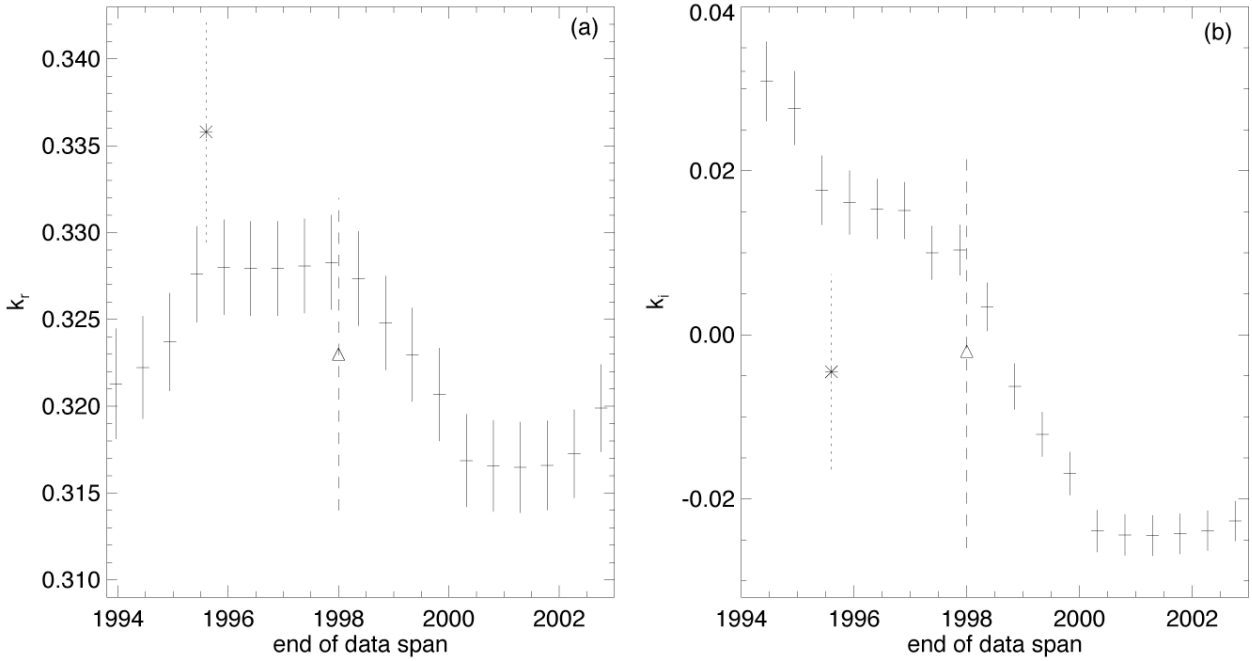

Figure 1. The real (a) and imaginary (b) parts of the 18.6-year body tide Love number k, obtained by fitting to subsets of *Cox et al's* [2003] SLR time series. Each subset uses SLR data between 1979 and a variable ending date, as specified on the x-axis. We summarize these results by adopting the values and uncertainties denoted by the triangles and accompanying error bars. The results from *Eanes* [1995] are shown as asterisks, for comparison.

Figure 1 shows that our CABC solutions have not yet converged to within the formal (plus ocean tide) errors. This is particularly true for the imaginary component, and is largely because of the anomalous post-1997 behavior of the SLR data. We summarize the CABC results by choosing k_r=0.323±0.009 and k_i=-0.002±0.024, shown as the triangles in Figure 1. These numbers lie midway between the 1996 and 2001 CABC values shown in Figure 1, and have uncertainties large enough to encompass the variations in both those parameter values.

Figure 2 compares the real and imaginary parts of the observed M_2 and 18.6-year Love numbers with the elastic results computed for the PREM seismic Earth model [*Dziewonski and Anderson,* 1981], using the methods described in *Wahr* [1981]. These elastic results are k_r=0.296 for the 18.6-year tide, k_r=0.299 for M_2, and k_i=0 for both the

18.6-year and M_2 tides. The M_2 observational results are shown as lines running along the k_r axis, because *Ray et al* [2001] were able to determine only the phase lag of the Love number. For both tides, the error bars have been expanded to include uncertainties in the ocean tide contributions (*Ray et al* included that uncertainty in their M_2 estimate; and for the 18.6-year tide we assumed the ocean tide uncertainty is 5% of the equilibrium model). Note that the observed values of k_r for the 18.6-year tide and of k_i for the M_2 tide, differ significantly from the elastic predictions. Presumably these discrepancies represent the effects of mantle anelasticity, through dissipation for the M_2 tide and dispersion for the 18.6-year tide.

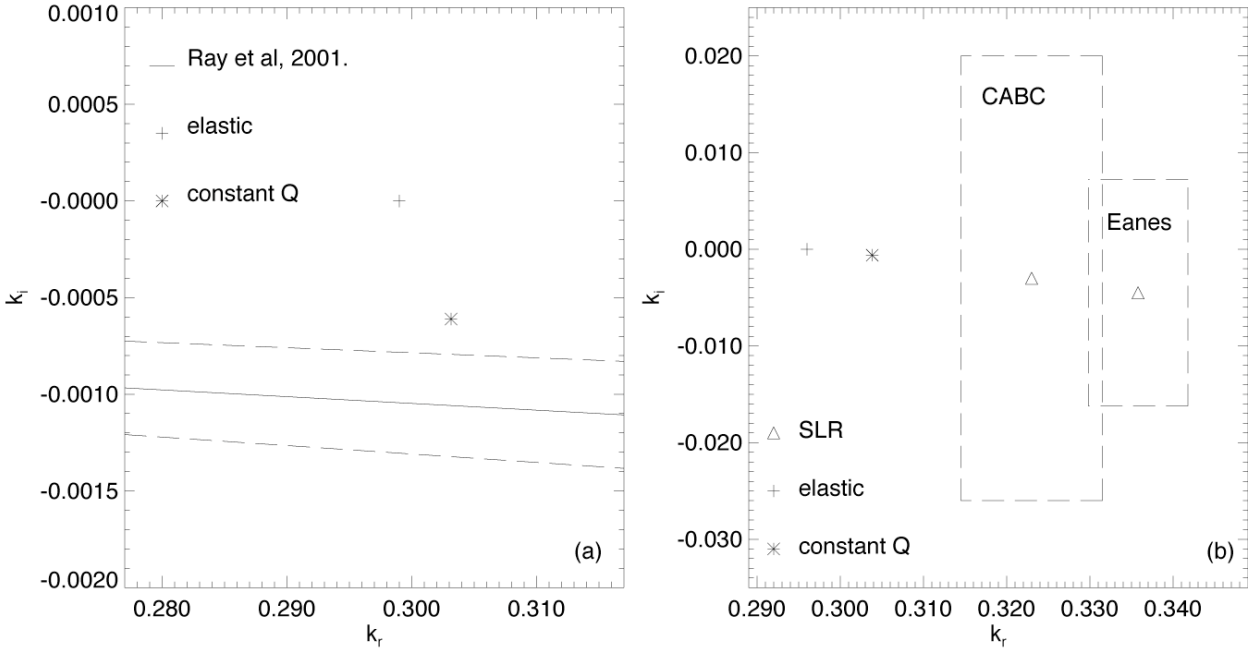

Figure 2. SLR body tide Love number results for the M_2 (a) and 18.6-year (b) tides, compared with predictions for an elastic Earth (plus signs) and for an anelastic Earth with a frequency-independent Q (asterisks). The dashed lines illustrate the errors in the recovered Love numbers. Two 18.6-year estimates are shown, one from *Eanes* [1995], and the other (CABC) based on data from *Cox et al* [2003].

Results for Anelasticity

Using the formulation of *Wahr and Bergen* [1986], we write the anelastic perturbation to the Love number k as:

$$\Delta k(\omega) = \int_{mantle} (\partial k(\omega)/\partial Q(r))\, \Delta Q(r)\, dr \qquad (6)$$

with ΔQ given by (5). There is a similar expression for the load Love number k'. We compute the partial derivative inside the integral numerically, by generating a solution for the Love number k using PREM, generating another solution obtained by slightly modifying the PREM shear modulus at radius r, and taking the difference.

Our objective is to place bounds on $\alpha(r)$ by comparing the SLR Love number solutions, after removing the predictions for an elastic Earth, with Love number estimates made using (6). Our two data points are not nearly sufficient to fully resolve this problem. So we make the following assumptions. First, we assume that α is independent of r, which is equivalent to assuming that the same physical mechanisms, with the same parameter values, are operative at all depths within the mantle. This is an over-simplification, and it probably tends to bias our recovered values of α towards the values of α operative in regions where Q is small (i.e., where the attenuation is large). Second, we choose ω_0 in (5) equal to 3.09×10^{-4}Hz. This is the frequency of the longest-period free oscillation

$_0S_2$, and is the smallest frequency within the seismic band. We assume that for $\omega<\omega_0$, the frequency dependence of Q is given by (4), and we choose different values of α to compare with the observations. But we assume that Q is independent of frequency for $\omega>\omega_0$. This is consistent with seismic observations and with the assumptions of PREM. Third, we use this second assumption to relate the reference values $Q_0(r)$ and $\omega_0(r)$ in (5), to the Q and ω values given in the seismic model PREM. We determine $Q_0(r)$ and $\omega_0(r)$ in the following way. The values of Q and ω tabulated in PREM are for a 1-second period. Consistent with our assumption of a frequency-independent Q at frequencies larger than $\omega_0=3.09\times10^{-4}$Hz, we use the PREM Q values for Q_0, and we use (5) in the $\omega\to 0$ limit to extrapolate the 1-sec PREM values of ω out to a frequency of ω_0. We use these extrapolated values as ω_0. By using the PREM values in this way we are, in effect, assuming that the mechanisms responsible for seismic dissipation are also responsible for the dissipation of the M_2 and 18.6-year tides.

Figure 3 compares the real and imaginary parts of the observed 18.6-year Love number and the imaginary part of the M_2 Love number, with our predictions based on (6) and (5). The elastic contributions as computed for PREM have been removed from the observations. The error bars on the observations of k_r have been increased over those shown in Figure 2, by adding (in quadrature) a possible 1% error in the elastic Love numbers. Our predictions are shown for five values of α: α = 0 (constant Q), 0.1,0.2,0.25, and 0.3. The observed values of k_r for the 18.6-year tide and of k_i for the M_2 tide, depart significantly from the predictions for a frequency-independent Q (α=0). This can also be seen in Figure 2. Instead, values of α between about 0.15 and 0.30 satisfy all observations. Note that the observed values of k_i for the 18.6-year tide are not constrained well enough to provide useful information on α.

We have repeated these comparisons, keeping Q fixed in the upper mantle (depths shallower than 660 km), while allowing the lower mantle Q to vary with frequency as described in (4). Our bounds on α are virtually unchanged. In contrast, keeping Q fixed in the lower mantle while allowing Q to vary with frequency in the upper mantle, requires much larger values of α. Thus, we interpret our result for α as a constraint primarily on lower mantle anelasticity.

Discussion

The SLR Love number values shown in Figures 2 and 3 are in clear disagreement with the predictions for an elastic Earth. In fact, they are in disagreement with predictions that assume Q is constant between the seismic band and these tidal frequencies (the α=0 case). There are many possible Q models that could explain the SLR results. We have hypothesized that the Q values for these tides can be obtained by extrapolating the seismic Q values to the tidal frequencies using a ω^{α} frequency dependence for Q. This is consistent with the assumption that the anelastic mechanisms are the same for tides as for seismic waves. The fact that the tidal and seismic results require different values of α is not necessarily inconsistent with this assumption, because no anelastic material can have a constant Q over all frequencies.

We find that α between 0.15 and 0.30 provides the best fit to our observations, and we conclude that this is primarily a bound on anelasticity in the lower mantle. In Figure 3 we also show results for the 14-month Chandler Wobble (CW) period and damping for three recent observational results [*Wilson and Vicente*, 1990; *Furuya and Chao*, 1996; and *Kuehne et al* 1996 (who obtained an estimate of the CW period, but not the damping)]. The CW results in Figure 3 have been corrected for an assumed equilibrium pole tide in the ocean (the response of the ocean to the centrifugal forces associated with the CW), and have been re-scaled so they can be directly compared with the real and imaginary parts of the tidal Love numbers. Note that the CW results are consistent with values of α in this same range.

Our solution for α depends on our choice of ω_0. If Q were truly constant throughout the entire seismic frequency band, then ω_0 could be no larger than the eigenfrequency of $_0S_2$ (corresponding to a period of about 54

minutes). But our decision to actually set ω_0 equal to this eigenfrequency is somewhat arbitrary. If we had chosen ω_0 to be smaller than this, our results for α would be even larger. In fact, if we choose ω_0 to be smaller than about 1 *cycle/6 hours*, there is no value of α that gives an acceptable fit to both the M_2 and 18.6-year results.

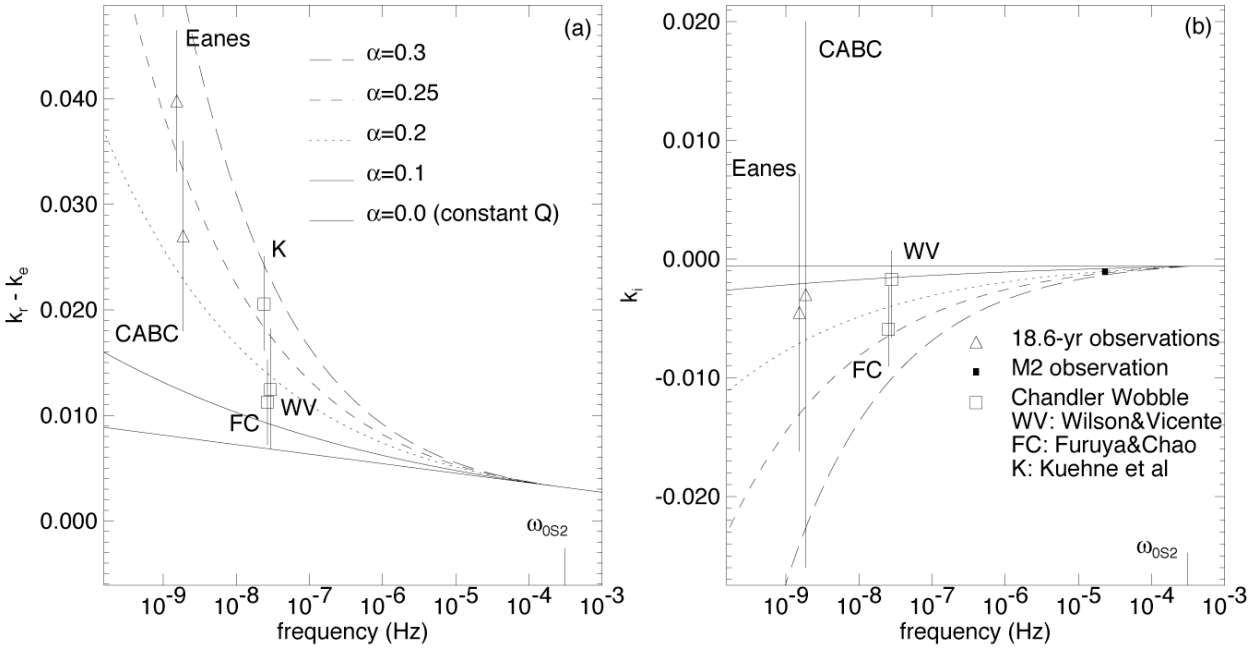

Figure 3. SLR Love number results with predictions for 5 anelastic models, each characterized by a different value of α in (5). For each model, α=0 at frequencies larger than $\omega_0 s_2$, the frequency of the longest-period seismic free oscillation. Panel (a) shows the real component (after removing the PREM elastic values) and so represents the effects of dispersion. Panel (b) shows the imaginary component, and so represents dissipation. Two 18.6-year estimates are shown, one from *Eanes* [1995], and the other (CABC) based on data from *Cox et al* [2003]. Results for three estimates of the Chandler Wobble period and damping are also shown, scaled so they can be compared to the real and imaginary components, respectively, of the body tide Love numbers.

Interestingly, although our preferred range for α is incompatible with the α =0 value required from seismology, it is in reasonable agreement with the upper mantle estimates of $\alpha \approx$0.15-0.40 inferred from laboratory experiments at seismic periods [see, for example, *Gribb et al*, 1998]. This agreement may be spurious, since our results are most sensitive to Q in the lower mantle rather than in the upper mantle. On the other hand, it could conceivably reflect a dependence of Q on stress amplitude. Stress amplitudes are on the order of 6×10^4 Pa for the M_2 tide, 3×10^3 Pa for the 18.6-year tide, and 2×10^2 Pa for the CW. To compare with seismic amplitudes, we note that the stress amplitude associated with the ${}_0S_2$ free oscillation, which has a radial structure that closely resembles that of the tidal and CW deformations, was on the order of 1 Pa following the magnitude 8.3, 1994 Bolivian earthquake, the largest deep earthquake ever recorded.

Thus, our tidal stresses are not only much larger than the most relevant seismic stresses, but are close to the stress levels employed in laboratory attenuation studies, which are typically on the order of 10^4 to 10^6 Pa. This suggests, though certainly does not prove, that the disagreement between the seismic and laboratory measurements of the frequency dependence of Q may be partially related to differences in stress amplitudes, rather than just to the difficulty in capturing the full complexity of mantle material within single laboratory samples.

Acknowledgments

We thank Chris Cox for providing his monthly SLR estimates of the Y_2^0 component of the Earth's gravity field, and we thank Chris Cox and Richard Eanes for helpful discussions. This work was partially supported by NASA grants NAG5-7703 and NGT5-50320 to the University of Colorado.

References

Carton, J.A., The variation with frequency of the long-period tides, *J. Geophys. Res., 88,* 7563-7571, 1983.

Cartwright, D.E., and R.J. Tayler, New Computations of the Tide-generating Potential, *Geophys. J.R. astr. Soc., 23*, 45-74, 1971.

Chao, B.F., and R.S. Gross, Changes in the Earth's rotation and low-degree gravitational field induced by earthquakes, *Geophys. J. R. Astron. Soc., 91,* 569-596, 1987.

Cox, C.M., A. Au, J.-P. Boy, and B.F. Chao, Time-variable gravity: Using satellite-laser-ranging as a tool for observing long-term changes in the Earth system, (this volume) , 2003.

Dahlen, F.A., and J. Tromp, *Theoretical Global Seismology*, Princeton University Press, 1025 pages, 1998.

Defraigne, P., and I. Smits, Length of day variations due to zonal tides for an inelastic earth in non-hydrostatic equilibrium, *Geophys. J. Int., 139,* 563-572, 1999.

Desai, S., and J. Wahr, Empirical Ocean Tide Models Estimated from TOPEX/Poseidon Altimetry, *J. Geophys. Res., 100 (C12)*, 25205-25228, 1995.

Desai, S., and J. Wahr, Monthly and fortnightly tidal variations of the Earth's rotation rate predicted by a TOPEX/Poseidon empirical ocean tide model, *Geophys. Res. Lett., 26*, 1035-1038, 1999.

Dickman, S.R., and Y.S. Nam, Constraints on *Q* at long periods from Earth's rotation, *Geophys. Res. Lett., 25*, 211-214, 1998.

Dziewonski, A,, and D.L. Anderson, Preliminary reference Earth model, *Phys. Earth Planet. Inter., 25*, 297-356, 1981.

Eanes, R.J., A study of temporal variations in Earth's gravitational field using LAGEOS-1 laser ranging observations, Ph.D. Thesis, Univ. of Texas at Austin, 128 pp, 1995.

Furuya, M., and B.F. Chao, Estimation of period and Q of the Chandler Wobble, *Geophys. J. Int., 127,* 693-702, 1996.

Gribb, T.T., and R.F. Cooper, Low-frequency shear attenuation in polycrystalline olivine: Grain boundary diffusion and the physical significance of the Andrade model for viscoelastic rheology, *J. Geophys. Res., 103,* 27,267-27,279, 1998.

Kuehne, J., C.R. Wilson, and S. Johnson, Estimates of the Chandler Wobble frequency and Q, *J. Geophys. Res., 101,* 13573-13579, 1996.

Ray, R.D., and D.E. Cartwright, Satellite altimeter observations of the Mf and Mm ocean tides, with simultaneous orbit corrections, in *Gravimetry and Space Techniques Applied to Geodynamics and Ocean Dynamics, Geophysical Monograph 82*, IUGG Volume 17, 69-78, 1994.

Ray, R.D., R.J. Eanes, and F.G. Lemoine, Constraints on energy dissipation in the Earth's body tide from satellite tracking and altimetry, *Geophys. J. Int., 144,* 471-480, 2001.

Smith, M.L., and F.A. Dahlen, The period and Q of the Chandler Wobble, *Geophys. J. R. astr. Soc., 64*, 223-282, 1981.

Wahr, J.M., Body tides on an elliptical, rotating, elastic and oceanless Earth, *Geophys. J. R. astr. Soc., 64*, 677-704, 1981.

Wahr, J.M., and Z. Bergen, The effects of mantle anelasticity on nutations, Earth tides, and tidal variations in rotation rate, *Geophys. J. Roy. Astr. Soc., 87*, 633-668, 1986.

Wilson, C.R., and R.O. Vicente, Maximum likelyhood estimates of polar motion parameters, in *Variations in Earth Rotation*, 151-156, D.D. McCarthy and W.E. Carter, eds., Geophysical Monograph 59, 1990.